Ultrafast magneto-optical response of iron thin films

T. Kampfrath* and R. G. Ulbrich
IV. Physikalisches Institut der Universität Göttingen, Bunsenstraße 13, D-37073 Göttingen, Germany

F. Leuenberger, M. Münzenberg, B. Sass, and W. Felsch
I. Physikalisches Institut der Universität Göttingen, Bunsenstraße 9, D-37073 Göttingen, Germany
(Received 22 October 2001; published 26 February 2002)

Optical pump probe techniques are utilized to measure the time-resolved magneto-optical Kerr effect (TRMOKE) of a ferromagnetic iron film at room temperature in air. We focus on the interpretation of the TRMOKE signal, and find the experimental data to be consistent with a simple phenomenological model. Nonmagnetic contributions are present in the TRMOKE signal up to 100 ps after excitation. Without making further assumptions, this prevents a determination of the true magnetization dynamics. The initial magnetization does not change its direction, and within the first picoseconds there is no detectable dependence of the magnetization dynamics on the external magnetic field.

DOI: 10.1103/PhysRevB.65.104429 PACS number(s): 75.40.Gb, 75.70.−i, 78.20.Ls, 78.47.+p

INTRODUCTION

The optical properties of solids depend on the solid's magnetic order. For example, if a *p*- or *s*-polarized light beam is incident onto a ferromagnetic metal surface the reflected light becomes elliptically polarized. The major axis of the resulting polarization ellipse is rotated by the Kerr angle θ out of the original polarization plane. The ellipticity and θ scale with the sample magnetization averaged over the probing region. This phenomenon is called the magneto-optical Kerr effect (MOKE), and has found many applications in studying equilibrium magnetic properties of thin films[1] and in data recording technology.[2] In addition, it can be observed in the medium's second-order response.[3]

Recently MOKE and its nonlinear version were employed to investigate magnetization dynamics of solids triggered by excitation with short magnetic-field pulses[4] or femtosecond laser pulses.[5–8] In the latter case all authors report an instantaneous decrease of the Kerr signal, but the interpretation of this time-resolved MOKE (TRMOKE) is heavily debated. Koopmans *et al.*[8] simultaneously measured the Kerr rotation and ellipticity of nickel films, and showed that the TRMOKE signal does *not* simply scale with magnetization during the first picosecond after excitation, as it does in the static case. Moreover, they consider an instantaneous demagnetization to be very unlikely. This is in clear contrast to the interpretation by Hohlfeld *et al.*[7] and to theoretical predictions by Zhang and Hübner.[9] Due to both fundamental and technological interest, further research is required to clarify this discrepancy.

EXPERIMENT

The experimental setup is shown schematically in Fig. 1. A commercial Ti:sapphire regenerative laser system provided 150-fs laser pulses with a center wavelength of 800 nm and a repetition rate of 250 kHz. The laser beam was split into pump and probe beams by a beam splitter. After passing a delay line, the linearly polarized pump beam was focused onto the sample surface at normal incidence. A spot diameter of 150 μm led to an incident pump fluence of 0.5 mJ/cm^2.

The probe beam—much weaker in intensity than the pump beam—was polarized by a Glan laser polarizer, and then focused onto the sample at an angle of incidence of 53°. The resulting spot diameter was about half as large as that of the pump beam, which guaranteed a homogeneously excited probing region. After reflection from the sample and collimation, the beam's Kerr rotation θ was detected through the use of a Wollaston prism splitting the incoming light into two beams polarized perpendicularly to each other. The photocurrents generated by these beams were subtracted from one another, and fed into a lock-in amplifier. The resulting voltage scaled linearly with θ, provided the two photocurrents were equalized with the pump beam blocked.[10] Moreover, proper equalization minimized the influence of pump-induced reflectivity changes of the sample. For measurements without a pump beam the probe beam was chopped mechanically at 800 Hz. Pump *and* probe measurements were performed with a modulated pump beam. Also, the probe beam wavelength could be changed to 400-nm employing optical second-harmonic generation in a beta barium borate crystal.

The sample used was a 200-nm-thick polycrystalline iron film grown on a silicon (100) substrate by argon-ion sputter-

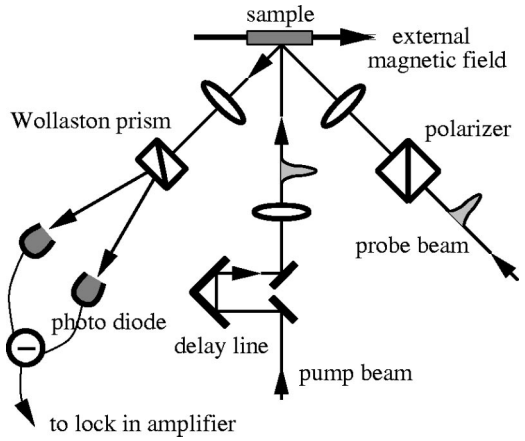

FIG. 1. Sketch of the experimental setup as seen from above.

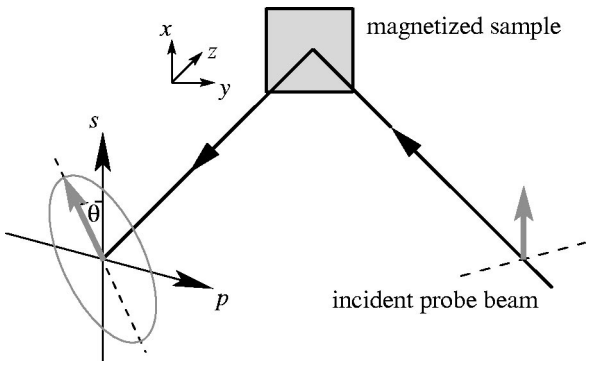

FIG. 2. Experimental situation and schematic of a reference frame with *x* and *y* axes pointing in transverse and longitudinal directions, respectively.

ing. The thickness was chosen to exclude interactions among the incident light beams and the substrate. In order to decouple the iron film growth from the substrate, a palladium buffer layer was used between the iron and silicon. A pair of Helmholtz coils generated an external magnetic field of up to 100 mT parallel to the plane of incidence and the sample surface. The obtained hysteresis loops were nearly rectangular with a coercive field of 5 mT. This implies that the sample was spontaneously magnetized preferentially in plane. The Kerr rotation covered a range of about 0.1° in a full hysteresis loop. A permanent magnet was used to magnetize the sample along the normal of the plane of incidence. We found the TRMOKE signal to be roughly proportional to the applied pump fluence, and independent of the pump beam's linear polarization.

SIMPLE MODEL

Koopmans *et al.*[8] discussed their TRMOKE data on the basis of microscopic models. Here a phenomenological track is taken by simply considering only effects up to first order in the sample magnetization. Before that we briefly review the phenomenological theory of the static MOKE. As shown in Fig. 2 a reflecting sample with magnetization $\boldsymbol{M}$ is hit by a probe beam with center frequency ω. The linear optical response of the sample is determined by its dielectric tensor $\underline{\epsilon}_\omega$.

Static case

The sample is in macroscopic equilibrium, having a magnetization $\boldsymbol{M}_0$. We assume the sample to be optically thick and homogeneous, and optically isotropic in the absence of any magnetization. The optical response of a ferromagnet is modified by the electron spins via spin orbit coupling. The latter can be considered as a small perturbation.[11,12] Therefore, it is often sufficient to restrict oneself to effects up to first order in $\boldsymbol{M}_0$. Beyond these there are magneto-optical effects of second order such as the Voigt effect,[13] which may contribute noticeably to the MOKE signal.[14] Nevertheless we linearize the dielectric tensor $\underline{\epsilon}_\omega(\boldsymbol{M}_0)$ in $\boldsymbol{M}_0$. Applying Onsager's relations leads to

$$\underline{\epsilon}_\omega(\boldsymbol{M}_0) = n_0^2 \mathbb{1} + \gamma_0 \boldsymbol{M}_0 \times ,$$

where n_0 is the sample's refractive index for vanishing magnetization. $\mathbb{1}$ and $\times$ denote the unity matrix and inner vector product, respectively. The magneto-optical coupling constant γ_0 indicates how strongly magnetism influences the sample's linear optical response. It is directly connected with the strength of spin-orbit coupling.[11,12] Solving Maxwell equations for this dielectric tensor up to first order in $\boldsymbol{M}_0$ results in the Kerr rotation

$$\theta_0 = \boldsymbol{a}_0 \cdot \boldsymbol{M}_0 + b_0 . \tag{1}$$

For perfectly *p*- or *s*-polarized incident light, one obtains $b_0 = 0$ and[15]

$$\left.\begin{matrix} \boldsymbol{a}_0^p \\ \boldsymbol{a}_0^s \end{matrix}\right\} = \mathrm{Re}\left[\frac{\cos\alpha}{\cos(\alpha \pm \beta)} \frac{\gamma_0}{(n_0^2 - 1) n_0} \begin{pmatrix} 0 \\ \tan\beta \\ \pm 1 \end{pmatrix} \right],$$

where α is the angle of incidence and β the complex angle of refraction determined by Snell's law. For an incident light beam with any linear polarization the quantity $\boldsymbol{a}_0$ is approximately a linear combination of $\boldsymbol{a}_0^p$ and $\boldsymbol{a}_0^s$. Additionally, an offset rotation b_0 can be observed because in general the Fresnel reflection coefficients r_{pp} and r_{ss} differ from one another.[16,15] Since the latter depend on the refractive index, the value of b_0 also does. Both $\boldsymbol{a}_0$ and b_0 are independent of $\boldsymbol{M}_0$ and any external magnetic dc field $\boldsymbol{B}_{\mathrm{ext}}$.[11,12] Up to first order in $\boldsymbol{M}_0$, there is no Kerr rotation for transverse magnetization because $a_{0x} = 0$.

Dynamic case

After the sample has been excited by the pump pulse its dielectric tensor becomes dependent on time *t*, and so does the Kerr rotation. Both are determined by the current values of $\boldsymbol{M}$ and other observables. Thus we start with the general ansatz

$$\theta(t) = f[\boldsymbol{M}(t), t]. \tag{2}$$

It is clear that the function *f* is modified when experimental conditions change, for example, parameters of the pump and probe pulses. Since considering effects up to first order in $\boldsymbol{M}$ was sufficient in the static case, we also linearize Eq. (2) in $\boldsymbol{M}$ and obtain

$$\theta(t) = \boldsymbol{a}(t) \cdot \boldsymbol{M}(t) + b(t).$$

This reduces to Eq. (1) when the sample has returned to its original macroscopic equilibrium state. Here $\boldsymbol{a}(t) = (\boldsymbol{\nabla}_{\boldsymbol{M}} f)(0,t)$ and $b(t) = f(0,t)$ are unknown phenomenological functions. Since they are independent of $\boldsymbol{M}_0$ and $\boldsymbol{B}_{\mathrm{ext}}$ in the static case we assume the same for the dynamical case. If the pump-induced changes of $\boldsymbol{M}$ and $\boldsymbol{a}$ are small compared to their static values $\boldsymbol{M}_0$ and $\boldsymbol{a}_0$, we finally obtain

$$\Delta\theta = \boldsymbol{a}_0 \cdot \Delta\boldsymbol{M} + \boldsymbol{M}_0 \cdot \Delta\boldsymbol{a} + \Delta b. \tag{3}$$

Obviously only the first contribution to the TRMOKE signal is proportional to the magnetization change, which is the

quantity of interest. The second term in Eq. (3) scales with the static magnetization, whereas the third one does not depend on $\boldsymbol{M}_0$. Remembering the facts about the static case, $\Delta \boldsymbol{a}$ and Δb are caused by pump-induced changes in the refractive index and the magneto-optical coupling constant, and by pump-induced optical anisotropies independent of the magnetization.

The probe pulse averages $\Delta\theta$ temporally and spatially over its finite duration and penetration volume, respectively. Following from Eq. (3), $\Delta \boldsymbol{M}$, $\Delta \boldsymbol{a}$, and Δb are averaged in the same way.

RESULTS

In this section we present the experimental data and show that it is consistent with the above introduced model.

Varying static magnetization and external field

According to the reference frame shown in Fig. 2, one has $\boldsymbol{M}_0=(0,M_0,0)$ for a longitudinally magnetized sample. We chose this configuration most frequently. It is reasonable to assume that reversal of $\boldsymbol{M}_0$ reverses the pump-induced $\Delta \boldsymbol{M}$, and rotating $\boldsymbol{M}_0$ by 90° around the sample's surface normal rotates $\Delta \boldsymbol{M}$ in the same manner. Written more formally, changing

$$\boldsymbol{M}_0 \rightarrow -\boldsymbol{M}_0 \quad \text{implies} \quad \Delta \boldsymbol{M} \rightarrow -\Delta \boldsymbol{M}, \tag{4}$$

and changing

$$\boldsymbol{M}_0 \rightarrow \boldsymbol{M}_0^{90^\circ} = \begin{pmatrix} -M_0 \\ 0 \\ 0 \end{pmatrix} \tag{5a}$$

implies

$$\Delta \boldsymbol{M} = \begin{pmatrix} \Delta M_x \\ \Delta M_y \\ \Delta M_z \end{pmatrix} \rightarrow \Delta \boldsymbol{M}^{90^\circ} = \begin{pmatrix} -\Delta M_y \\ \Delta M_x \\ \Delta M_z \end{pmatrix}. \tag{5b}$$

Rotating $\boldsymbol{M}_0$ into a transverse direction simply exchanges the roles of ΔM_x and ΔM_y.

Figure 3 shows TRMOKE curves recorded for various values of static magnetization and external magnetic fields. In the longitudinal configuration the Kerr signal drops within 200 fs after the sample's excitation by the pump pulse. This agrees with previous reports.[5–8] After a decay, $|\Delta\theta|$ starts to rise again slightly, and reaches a second maximum on a time scale of 10 ps. One sees that the TRMOKE curves are not completely inverted after reversal of the static magnetization. Nevertheless the sum curves are identical for all shown data in agreement with our model: Combining Eqs. (3) and (4) yields

$$\Delta\theta(\boldsymbol{M}_0) + \Delta\theta(-\boldsymbol{M}_0) = 2\Delta b$$

which is independent of $\boldsymbol{M}_0$ and $\boldsymbol{B}_{\text{ext}}$. The sum curves were sensitive to small changes of the incident probe beam's linear polarization. Moreover, they could be made to disappear in this way, that is, $\Delta b = 0$. In this case, the probe beam was most likely perfectly *p* polarized. Thus its polarization was not influenced by the temporally changing Fresnel reflection coefficient r_{ss}, leading to $b=0$. We conclude that magnetization-independent pump-induced optical anisotropies are negligible.

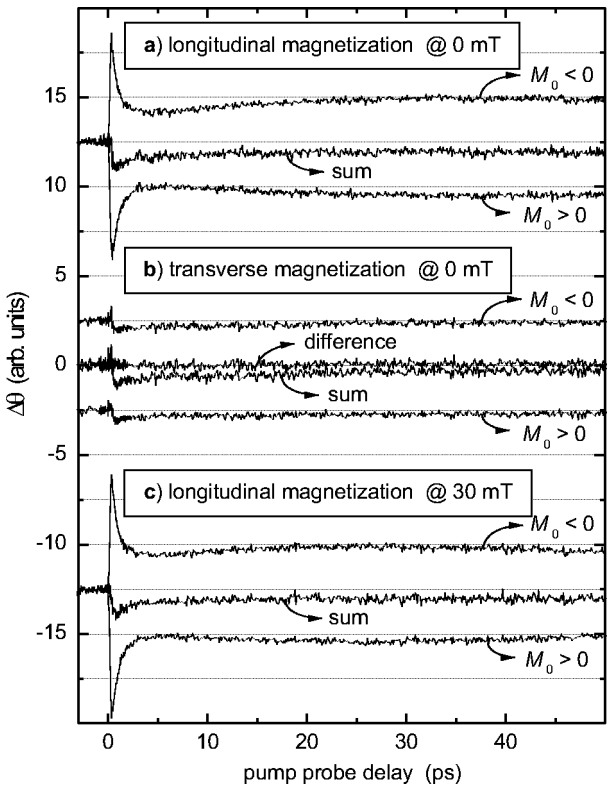

FIG. 3. TRMOKE curves for a *p*-polarized probe beam and a sample magnetized (a) remanently in the longitudinal direction, (b) remanently in transverse direction, and (c) by a 30-mT external field in the longitudinal direction. Sum curves for the opposite static magnetization and difference curves for the transverse configuration are also shown. Data are offset for clarity.

Taking the difference of the TRMOKE signals measured for opposite static magnetization eliminates Δb. Using $a_{0x}=0$ and Eqs. (3) and (5), we calculate this difference for the transverse configuration and obtain

$$\Delta\theta(\boldsymbol{M}_0^{90^\circ}) - \Delta\theta(-\boldsymbol{M}_0^{90^\circ}) = a_{0y}\Delta M_x + a_{0z}\Delta M_z - M_0 \Delta a_x .$$

As shown in Fig. 3(b), in this case the experimental difference signal vanishes for *all* pump-probe delays. Thus we can conclude from the last relation that most likely ΔM_x, ΔM_z, and Δa_x vanish as well. This is a plausible result. For reasons of symmetry only M_y should change in the longitudinal configuration. The vanishing Δa_x is in line with $a_{0x}=0$. It seems that there is no transverse MOKE in the dynamic case, either.

Varying probe beam wavelength and polarization

Combining Eqs. (3) and (4) and the above-mentioned result $\Delta M_z = 0$, we calculate the relative TRMOKE signal for the longitudinal configuration:

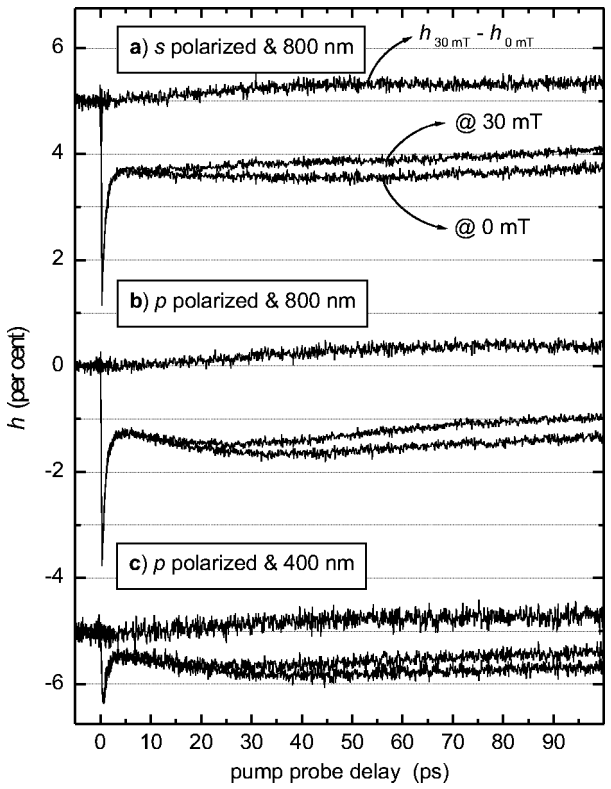

FIG. 4. TRMOKE curves for external magnetic fields of 0 and 30 mT measured with (a) an *s*-polarized probe beam at an 800-nm wavelength, (b) *p*-polarized probe beam at an 800-nm wavelength, and (c) *p*-polarized probe beam at a 400-nm wavelength. The differences between the 0- and 30-mT curves are also shown. Data are offset for clarity.

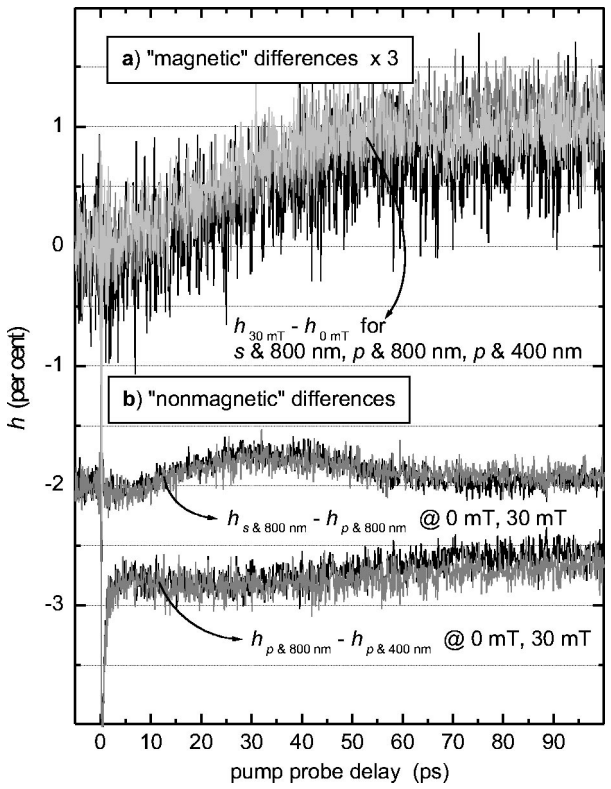

FIG. 5. Differences between *h* curves for (a) external magnetic fields of 0 and 30 mT and (b) various probe beam wavelengths and polarizations. Data in (a) and (b) are shown for various probe beam parameters and various external magnetic fields, respectively, and offset for clarity.

$$h := \frac{\Delta\theta(\boldsymbol{M}_0) - \Delta\theta(-\boldsymbol{M}_0)}{\theta_0(\boldsymbol{M}_0) - \theta_0(-\boldsymbol{M}_0)} = \frac{\Delta M_y}{M_0} + \frac{\Delta a_y}{a_{0y}}. \tag{6}$$

One recognizes purely magnetic and purely nonmagnetic contributions to this quantity. The magnetic contribution $\Delta M_y / M_0$ should be independent of the incident probe beam's wavelength and linear polarization. On the other hand the nonmagnetic quantity $\Delta a_y / a_{0y}$ should not be affected by the magnetization dynamics and the external magnetic field. These facts suggest the following experiment in order to provide another check of our model. TRMOKE curves were recorded for external magnetic fields of 0 and 30 mT. Each measurement was performed with *p*- and *s*-polarized probe beams at 800-nm wavelength and a *p*-polarized probe beam at 400-nm wavelength.

Figures 4(b) and 4(c) show that experimental *h* curves differ considerably for different probe beam wavelengths. Nevertheless, following Eq. (6), the difference

$$h_{30\,\mathrm{mT}} - h_{0\,\mathrm{mT}} = \left.\frac{\Delta M_y}{M_0}\right|_{30\,\mathrm{mT}} - \left.\frac{\Delta M_y}{M_0}\right|_{0\,\mathrm{mT}} \tag{7}$$

should be independent of the probe beam wavelength and polarization. As can be seen in Fig. 5(a), this agrees well with experimental data. Looking at Eq. (7) we conclude that $h_{30\,\mathrm{mT}} - h_{0\,\mathrm{mT}}$ really displays the difference between the magnetization dynamics of the sample in a 30-mT external field and the magnetization dynamics of the sample without an external field. Since this truly ''magnetic'' difference is zero within the first picoseconds after excitation, an external magnetic field does *not* play any significant role for the magnetization dynamics during this period of time. This finding can be understood by the following energetic argument. Within the first few hundred femtoseconds after excitation, a significant part of the absorbed pump pulse energy is still deposited in the electron system of the probing region.[17] This additional kinetic energy is large compared to the potential energy of the electron spins in the applied external magnetic field, and dominates the dynamics. The external field increases its influence with the amount of heat which has already left the electron system of the probing region.

From the ''magnetic'' difference curves we derive a lower bound to the pump-induced magnetization change. For this purpose we apply the relation $|a-b| \leqslant 2\max\{|a|,|b|\}$ to Eq. (7), and obtain

$$\max\left\{\left|\frac{\Delta M_y}{M_0}\right|_{0\,\mathrm{mT}}, \left|\frac{\Delta M_y}{M_0}\right|_{30\,\mathrm{mT}}\right\} \geqslant \frac{1}{2}\left|h_{30\,\mathrm{mT}} - h_{0\,\mathrm{mT}}\right|.$$

Looking at Fig. 5(a), we estimate a value of 0.1% for the right side of this inequality for pump probe delays from 60 to 100 ps. We infer a relative magnetization change of at least 0.1%.

The finding $h_{30\,\mathrm{mT}}-h_{0\,\mathrm{mT}}\geqslant 0$ is plausible. Assuming that $|M_{0y}|$ is not increased, $\Delta M_y/M_{0y}\leqslant 0$, and using Eq. (7), this leads to

$$\left.\frac{\Delta M_y}{M_0}\right|_{0\,\mathrm{mT}} \leqslant \left.\frac{\Delta M_y}{M_0}\right|_{30\,\mathrm{mT}} \leqslant 0.$$

An external magnetic field parallel to $\boldsymbol{M}_0$ supports the restoration of the original magnetization.

Instead of the above mentioned ''magnetic'' differences one can also consider ''nonmagnetic'' differences such as

$$h_{p\&800\,\mathrm{nm}}-h_{p\&400\,\mathrm{nm}}=\left.\frac{\Delta a_y}{a_{0y}}\right|_{p\&800\,\mathrm{nm}}-\left.\frac{\Delta a_y}{a_{0y}}\right|_{p\&400\,\mathrm{nm}}. \quad (8)$$

It should be independent of static magnetization and external magnetic field. This assertion is equivalent to the statement that difference (7) is independent of the probe beam wavelength. Thus the identical difference curves for different external magnetic fields in Fig. 5(b) are not surprising. If there were only magnetic contributions to the TRMOKE signal, difference (8) would have to be zero. Figure 5(b) shows that this is not the case. We conclude that nonmagnetic contributions considerably affect the TRMOKE signal during the first 2 ps after excitation.

As pointed out by Koopmans *et al.*[8] the nonmagnetic TRMOKE contributions are due to the redistribution of electrons in phase space. This results in different bleaching effects for left and right circularly polarized probe light, and leads to a Kerr rotation which is *not* caused by any magnetization change. Instead of comparing the transient Kerr rotation for different probe beam wavelengths, Koopmans *et al.*[8] considered Kerr rotation and ellipticity at the same wavelength. Their ''nonmagnetic'' difference $h_{\mathrm{rotation}}-h_{\mathrm{ellipticity}}$ is clearly nonzero within the first few hundred femtoseconds after excitation, but vanishes within 1 ps. In contrast, our ''nonmagnetic'' difference [Eq. (8)] is nonzero for a much longer time. On the one hand, this behavior might arise because different photon energies probe different optical transitions and thus react differently to the modified electron distributions. On the other hand, the sample of Koopmans *et al.*[8] was a single crystalline nickel film on a copper substrate, and cannot be directly compared to our much thicker polycrystalline iron film on a silicon substrate.

DISCUSSION

As shown in the previous sections, the normalized TRMOKE signal h is the sum of the two unknown quantities $\Delta a_y/a_{0y}$ and $\Delta M_y/M_0$. Thus a single h measurement is not sufficient to extract the sample's magnetization dynamics. To achieve this one has to measure the TRMOKE for a new set of experimental parameters without modifying the magnetization dynamics $\Delta M_y/M_0$. As an example, one could choose another probe beam wavelength, polarization, or angle of incidence. But then the nonmagnetic contribution $\Delta a_y/a_{0y}$ changes in an unknown way, and again there are not enough data to determine the sample's magnetization dynamics. Further assumptions concerning the nonmagnetic contribution are necessary to provide the missing information. This seems to be a difficult task especially during the first picosecond after excitation since it requires all microscopic details of the sample.

The phenomenological ansatz [Eq. (2)] and its consequences should not only be valid for the Kerr rotation θ but also for other observables such as Kerr ellipticity and the second-harmonic intensity generated by the probe beam. Therefore, in principle all linear and nonlinear TRMOKE techniques[5–8] suffer from the influence of nonmagnetic artifacts which are not easily negligible.

For a similar reason care should be taken when temperature induced demagnetization is measured with MOKE. Nonmagnetic contributions induced by the temperature change might superimpose the true demagnetization curve noticeably.

CONCLUSION

We have shown our experimental TRMOKE data to be consistent with a simple phenomenological model. The TRMOKE signal is influenced by nonmagnetic contributions which prevent the determination of the sample's magnetization dynamics. This is especially true for the first few hundred femtoseconds after excitation. Only the difference between two magnetization dynamics—induced by different external magnetic fields—can be considered. Since an external magnetic field does not play any detectable role within the first picosecond, no information about the ultrafast magnetization change can be obtained.

ACKNOWLEDGMENTS

We thank M. Hübner for contributions during the early stage of this work, and gratefully acknowledge R. Ziebold, U. Bovensiepen, A. Grujic, A. Müller, and D. Starr for fruitful and enlightening discussions. This work was supported by the Deutsche Forschungsgemeinschaft, Sonderforschungsbereich 345.

*Electronic address: tobias.kampfrath@physik.fu-berlin.de

[1] Z. Q. Qiu and S. D. Bader, Rev. Sci. Instrum. **71**, 1243 (2000).
[2] M. Mansuripur, *The Physical Principles of Magneto-Optical Recording* (Cambridge University Press, Cambridge, 1995).
[3] *Nonlinear Optics in Metals*, edited by K. H. Bennemann (Oxford University Press, Oxford, 1998).
[4] A. Y. Elezzabi, M. R. Freeman, and M. Johnson, Phys. Rev. Lett. **77**, 3220 (1996).
[5] E. Beaurepaire, J.-C. Merle, A. Daunois, and J.-Y. Bigot, Phys. Rev. Lett. **76**, 4250 (1996).
[6] G. Ju, A. Vertikov, A. V. Nurmikko, C. Canady, G. Xiao, R. F. C. Farrow, and A. Cebollada, Phys. Rev. B **57**, 700 (1998).
[7] J. Hohlfeld, E. Matthias, R. Knorren, and K. H. Bennemann, Phys. Rev. Lett. **78**, 4861 (1997); **79**, 960 (1997).
[8] B. Koopmans, M. van Kampen, J. T. Kohlhepp, and W. J. M. de Jonge, Phys. Rev. Lett. **85**, 844 (2000).

[9] G. P. Zhang and W. Hübner, Phys. Rev. Lett. **85**, 3025 (2000).
[10] J. Schoenes, in *Materials Science and Technology*, edited by R. W. Cahn, P. Haasen, and E. J. Kramer (VCH Weinheim, 1992), Vol. 3A.
[11] P. N. Argyres, Phys. Rev. **97**, 334 (1955).
[12] H. S. Bennett and E. A. Stern, Phys. Rev. **137**, 448 (1965).
[13] P. S. Pershan, J. Appl. Phys. **38**, 1482 (1967).
[14] K. Postava, H. Jaffres, A. Schuhl, F. N. van Dau, M. Goiran, and A. R. Fert, J. Magn. Magn. Mater. **172**, 199 (1997).
[15] C.-Y. You and S.-C. Shin, J. Appl. Phys. **84**, 541 (1998).
[16] M. Born and E. Wolf, *Principles Of Optics* (Pergamon Press, Oxford, 1983).
[17] J. Hohlfeld, S.-S. Wellershoff, J. Güdde, U. Conrad, V. Jähnke, and E. Matthias, Chem. Phys. **251**, 237 (2000).